solutes passing through the column is dependent on the interaction or displacement of the acetonitrile, rather than displacement of hydrogen-bonded water on the silica gel surface. The mass of the three solvents produces a stable and self-activating chromatographic system in equilibrium. The presence of 1% ethanol or methanol, commonly used preservatives in chloroform and methylene chloride, does not adversely affect retention times or resolution of the solutes.

REFERENCES

(1) W. E. Juhl and R. D. Kirchhoefer, *J. Pharm. Sci.*, **69**, 544 (1980).

(2) R. D. Kirchhoefer and W. E. Juhl, *J. Pharm. Sci.*, **69**, 548 (1980).

(3) R. D. Kirchhoefer, J. C. Reepmeyer, and W. E. Juhl, *J. Pharm. Sci.*, **69**, 550 (1980).

(4) R. D. Kirchhoefer, *J. Pharm. Sci.*, **69**, 1188 (1980).

(5) *Pharmacopeal Forum*, **6**(5), 414 (1980).

(6) P. P. Ascione and C. P. Chrekian, *J. Pharm. Sci.*, **64**, 1029 (1975).

(7) R. G. Baum and F. F. Cantwell, *J. Pharm. Sci.*, **67**, 1066 (1978).

(8) P. J. Twitchett, A. E. P. Gorvin, and A. C. Moffat, *J. Chromatogr.*, **120**, 359 (1976).

(9) D. Blair, B. H. Rumack, and R. G. Peterson, *Clin. Chem.*, **24**, 1543 (1978).

(10) R. L. Stevenson and C. A. Burtis, *J. Chromatogr.*, **61**, 253 (1971).

(11) V. D. Gupta, *J. Pharm. Sci.*, **69**, 110 (1980).

(12) V. D. Gupta, *J. Pharm. Sci.*, **69**, 113 (1980).

(13) G. W. Peng, M. A. F. Gadalla, V. Smith, A. Peng, and W. L. Chiou, *J. Pharm. Sci.*, **67**, 710 (1978).

(14) S. L. Ali, *J. Chromatogr.*, **126**, 651 (1976).

(15) H. Bundgaard, *Arch. Pharm. Chem., Sci. Ed.*, **4**, 103 (1976).

(16) C. D. Pfeiffer and J. W. Pankey, *J. Pharm. Sci.*, **71**, 511 (1982).

(17) R. N. Galante, J. C. Egoville, A. J. Visalli, and D. M. Patel, *J. Pharm. Sci.*, **70**, 167 (1981).

(18) R. P. W. Scott, *J. Chromatogr. Sci.*, **18**, 297 (1980).

(19) R. P. W. Scott and P. Kucera, *J. Chromatogr.*, **149**, 93 (1978).

(20) R. P. W. Scott and P. Kucera, *J. Chromatogr.*, **171**, 37 (1979).

Particle Size and Surface Area Distributions of Pharmaceutical Powders by Microcomputerized Mercury Porosimetry

F. CARLI ˣ **and A. MOTTA**

Received June 1, 1982, from the *Physical Pharmacy Laboratory, Pharmaceutical Research and Development, Farmitalia Carlo Erba, Milan, Italy.* Accepted for publication December 16, 1982.

Abstract □ The Mayer–Stowe theory was applied to derive the particle size distribution of powders of pharmaceutical interest using mercury porosimetry. Particle size data obtained by this approach are fairly comparable with data derived by other, more popular, techniques such as the electrical sensing zone or the air jet sieving methods provided that the experimental value of the mercury–powder contact angle and the state of aggregation of the powder are carefully studied. Furthermore, by applying the Rootare–Prenzlow method a surface area distribution can also be derived from the same porosimetry data used to obtain the particle size distribution. All experiments were carried out with a microcomputerized mercury porosimeter, which allows storage of data during the analysis and a subsequent fast elaboration at the end of the run, with fully printed data on pore size, pore volume, surface area, and particle size of the powder sample.

Keyphrases □ Mercury porosimetry—application to particle size and surface area distributions, pharmaceutical powders □ Particle size—distribution in pharmaceutical powders, determination by mercury porosimetry □ Surface area—particles in pharmaceutical powders, distribution, determination by mercury porosimetry

The particle size of pharmaceutical powders plays a major role both in drug processing and bioavailability. Poorly soluble drugs are often rendered more available for absorption by reducing the particle size, *i.e.*, increasing the surface area (1–3). On the other hand, very important technological processes such as the compression (4) or mixing of powders (5) are strongly influenced by the particle size of the materials used. Not only the powdered drugs, but also the excipients, exhibit many particle size- or surface area-related properties. For example, (a) the lubricating efficacy of materials such as magnesium stearate is strongly influenced by the surface area of the powder (6), and (b) the disintegrating properties of povidone derivatives are dependent on particle size (7).

The growing need for particle size and surface area analyses has led to the introduction of such methods for particle size analysis as microscopic counting (8), the electrical sensing zone method (8, 9), the air jet sieving technique (8, 10), and simple sieving (8). The surface area analysis methods used range from gas adsorption techniques (11, 12) to gas diffusion or permeability (6).

Although mercury porosimetry is used mostly to characterize the porous structure of materials (13, 14), it has been used to determine the surface area (15) and the particle size of powders, both in the coarse region (16, 17) and in the submicron range (18). In pharmaceutics mercury porosimetry has been used almost exclusively to study the porous structure of tablets (19–21), granules (22, 23), or polymeric matrices (24, 25); no attempt has been made to characterize the micromeritics of pharmaceutical powders (26). In this paper, we use mercury porosimetry to measure the particle size and the surface area distributions of powdered drugs and excipients.

THEORETICAL

Particle Size Determination—The mercury porosimetry principle, based on the Washburn model, consists of registering the volume of pores penetrated at each intrusion pressure, which can be easily transformed into pore size *via* the Washburn equation (27) to give a complete pore size distribution. An alternative model describing the penetration of mercury was proposed by Frevel and Kressley (28) and subsequently developed by Mayer and Stowe (29). This treatment defines the solid being pene-

0022-3549/84/0200-0197$01.00/0

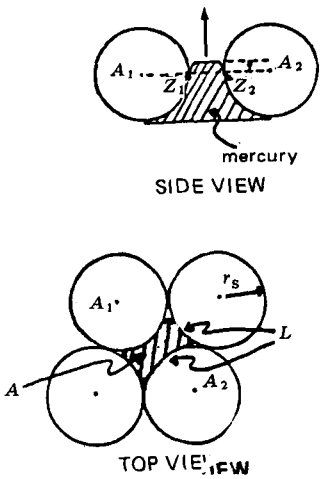

Figure 1—*Mayer–Stowe model for mercury intrusion between spherical particles. Breakthrough pressure (P) = $\gamma(L'/A)/r_s$, where γ is the surface tension of mercury, L′ is a parameter related to the cross-sectional perimeter (L) of mercury, A is the cross-sectional area of mercury at Z_1, Z_2, and r_s is the particle radius.*

trated by mercury as an assembly of spherical particles, packed together, and relates the size of the access opening to the radius of the spherical particles, rather than that of the cylindrical pore as in the case of the Washburn model.

The basic equation of the Mayer–Stowe model is given by:

$$P = \gamma \frac{(L')}{A} \Big/ r_s \qquad \text{(Eq. 1)}$$

where P is the intrusion or "breakthrough" pressure, r_s is the particle radius, L' is a parameter related to the perimeter L of the cross section of mercury intruding the touching spheres, A is the area of the cross section of intruding mercury, and γ is the surface tension of mercury (Fig. 1). The term L'/A is a function of the packing angle of the powder bed and the mercury contact angle. Mayer and Stowe calculated this ratio for all the possible packing angles originated by powder bed porosities in the range of 0.25–0.48 and contact angles from 180° to 100°; L'/A values calculated at 0.48 porosity can be extended to higher porosities, as stressed also by Stanley-Wood (18). Thus, once the correct L'/A value is chosen from the Mayer–Stowe table (29), one is able to directly derive from the experimental intrusion pressure the radius of the spherical particles originating the voids which are penetrated by mercury. At each intrusion pressure the mercury penetration volume is also registered; by expressing the volume as a percentage of the overall penetration volume measured at the end of the run, it is possible to derive a complete particle size distribution on a volume basis (16).

Surface Area Determination—Surface area values are usually derived by mercury porosimetry data assuming that pores are cylindrical (30, 31); at each intrusion pressure the mercury volume registered can be used to obtain a rough evaluation of the surface area of the pore walls by a simple geometrical calculation. An alternative model, based on no geometrical assumption and thus very much more reliable, has been developed by Rootare and Prenzlow (15). Their approach considers the process of mercury penetration from an energy point of view and leads to the following equation describing the work necessary to cover an infinitesimal area dA of a powder surface with mercury:

$$\gamma \cos \vartheta \cdot dA = -P \cdot dV_i \qquad \text{(Eq. 2)}$$

Where γ is the surface tension of mercury, ϑ is the mercury contact angle, dA is an infinitesimal area of powder surface, P is the intrusion pressure, and dV_i is the infinitesimal intrusion volume. The left-hand term of Eq. 2 is the work of immersion of the infinitesimal area dA into mercury and the right-hand term is the work effectively exerted by the mercury porosimeter in the course of the intrusion run.

Integration of Eq. 2 leads to:

$$A = \int dA = -\frac{1}{\gamma \cos \vartheta} \int_{V_0}^{V_{max}} P \cdot dV_i = -\frac{1}{\gamma \cos \vartheta} \int_{0}^{V_{max}} P \cdot dV_i \qquad \text{(Eq. 3)}$$

where A is the powder surface area, V_0 is the intrusion volume registered at $P = 0$ (*i.e.*, is equal to 0), and V_{max} is the final overall volume of mercury intrusion. Equation 3 may be used as a basis not only for calculating a total surface area from mercury porosimetry data, but also a surface area distribution on a particle size basis. In fact, at each intrusion pressure it is possible, on one side, to calculate the partial contribution to the overall value of the integral in Eq. 3 and, on the other side, to calculate from the P value the corresponding particle size value *via* Eq. 1.

EXPERIMENTAL

Materials—The powdered drugs used were indoprofen[1] (an organic weak acid) a morpholine derivative (drug A)[1], and an ergoline derivative (drug B)[1]. The other powders used were barium sulfate[1], cross-linked povidone[2], crystalline lactose[3], microcrystalline cellulose[4], magnesium stearate[1], and fumed silica[5]. All powders were used as received.

Mercury Porosimetry—Particle size and surface area analyses were carried out using a high-pressure mercury porosimeter[6], with intrusion pressures ranging from 1 to 2000 kg/cm^2, and with a low-pressure porosimeter[7], with pressure ranging from 0 to 3.5 kg/cm^2. The porosimeter was connected *via* an interface data logger[8] to a microcomputer[9] and a printer–plotter unit[8].

The powder samples (typical weights ranged from 100 to 300 mg) were introduced as received, in the dry state, into the sample container and then into the low-pressure porosimeter, where they were deaerated. The mercury penetration volume was subsequently registered while the intrusion pressure was increased to atmospheric pressure. The sample container was removed from the low-pressure unit and placed inside the high-pressure porosimeter; mercury penetration volume was registered while intrusion pressure was increased to 2000 kg/cm^2.

Mercury–Powder Contact Angle—Mercury–powder contact angles were measured by means of a wettability tester[10] using the method of Mack (32). Dimensions of the mercury droplets on the surface of a compact prepared with the sample powder were taken after increasing the droplet volume; thus, the derived contact angle can be considered as an advancing one (33). This seems to be the most correct value to be used in intrusion mercury runs (34), especially in loose powder beds, although some uncertainty remains (35). At least 10 replicates were carried out.

Electrical Sensing Zone Method—Particle size analyses were also carried out with an electrical sensing zone apparatus[11]. The suspension liquid used was 0.85% NaCl aqueous solution containing 0.1% surfactant. If necessary, this solution was saturated with the powder under examination. Disaggregation of the sample was further induced by sonicating the suspension. Orifice tubes of different size were used, allowing the determination of particles ≥ 0.6 μm.

Air Jet Sieving Technique—Particle size analyses by the air jet sieving technique were carried out with an air jet sieve[12]. The smallest detectable particle size was 32 μm.

Surface Area Determination by Gas Diffusion—Surface area analyses were carried out using a gas diffusion apparatus[13]. Powder samples were packed into the diffusion cell, and then helium was allowed to flow through the sample. From the rate of gas pressure decay, a surface area value was derived *via* a modified Knudsen equation (36).

Powder Density—The densities of the powders were measured with an air-comparison pycnometer[14].

RESULTS AND DISCUSSION

Mercury intrusion curves for crystalline lactose, microcrystalline cellulose, indoprofen, and magnesium stearate powders are shown in Fig. 2A–D, respectively. The particle size distribution for these powders are given in Figs. 3A–D.

Particle Size Determination—*Lactose*—In Fig. 2A, the mercury intrusion curves into a powdered sample of the widely used diluent crystalline lactose is shown. Curve A (the first mercury intrusion registered) presents a sharp increase in a very low range (0.1–1 kg/cm^2) of

[1] Farmitalia Carlo Erba, Italy.
[2] GAF.
[3] DMV, The Netherlands.
[4] Avicel PH 105, FMC Corp.
[5] Degussa, Germany.
[6] Model 200; Carlo Erba Strumentazione, Italy.
[7] Macropore Unit; Carlo Erba Strumentazione, Italy.
[8] Adcomp, Germany.
[9] Model CBM 4032; Commodore.
[10] Lorentzen-Wettre, Sweden.
[11] Coulter Counter Model TA II, Coulter Electronics, UK.
[12] Alpine, Germany.
[13] Alstan Diffusion Surface Area Meter, Powder Characterization Systems, U.K.
[14] Beckman.

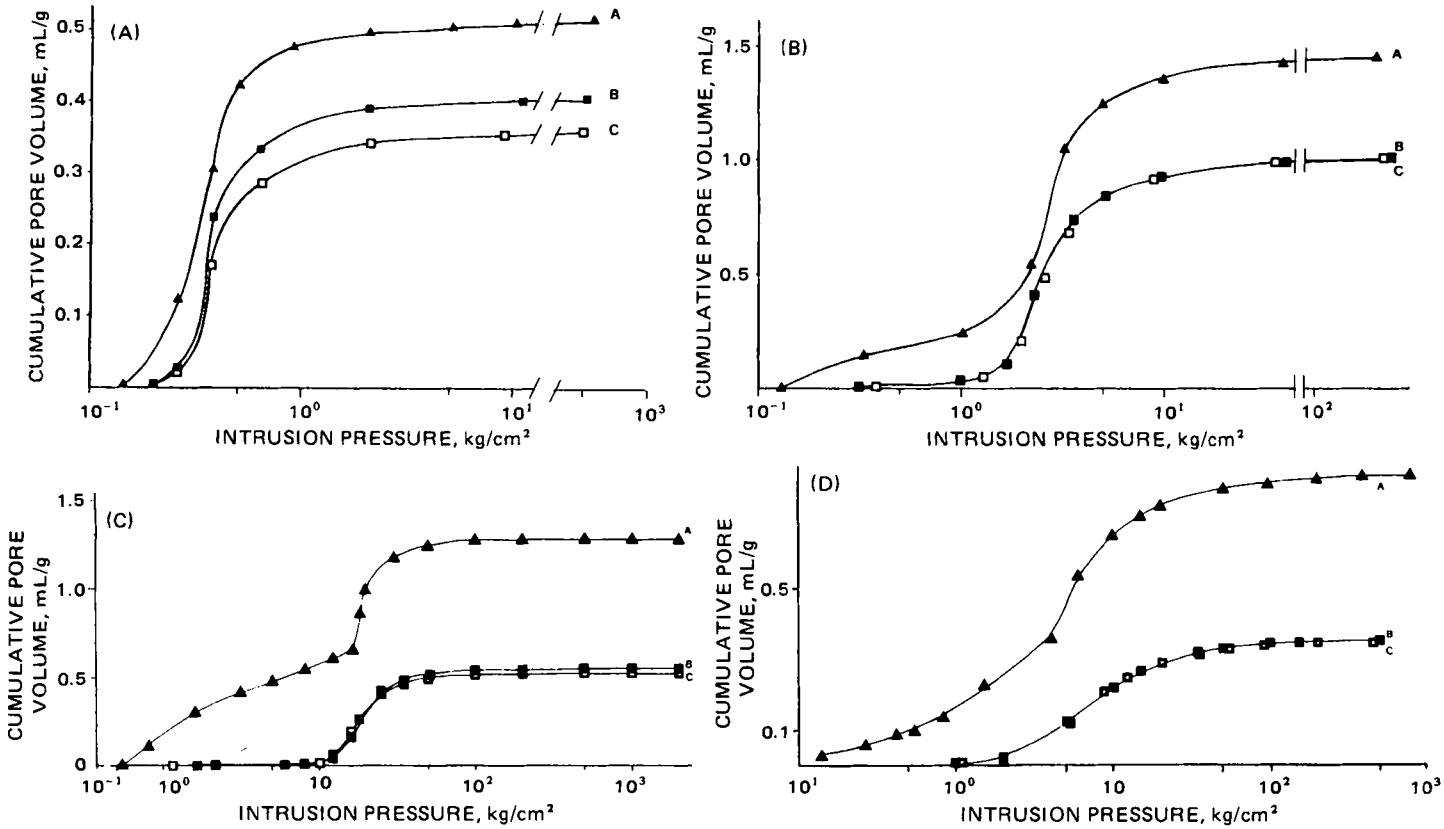

Figure 2—*Mercury intrusion of crystalline lactose (A), microcrystalline cellulose (B), indoprofen (C), and magnesium stearate (D) powders. Key: (▲) first run; (■) second run; (□) third run.*

pressures followed by a constant plateau value, suggesting the presence only of large interparticle voids. From the final overall volume of mercury penetration, the powder bed porosity is calculated by (18):

$$\epsilon = \frac{V_{max}}{V_{max} + 1/d} \qquad \text{(Eq. 4)}$$

where ϵ is the powder bed porosity, V_{max} is the final overall mercury intrusion volume, and d is the density of the powder sample. Once the ϵ value is calculated (in the case of the first run ϵ was 0.44), one can derive the powder bed packing angle σ from the Mayer and Stowe paper (Table 2 of Ref. 29) and subsequently obtain the L'/A value using the σ value and the experimental contact angle (Table 3 of Ref. 29). For lactose, the mercury contact angle was 144°.

The mercury intrusion pressures of Fig. 2A can be transformed into particle size *via* Eq. 1, and the mercury intrusion volumes expressed as percentages of the total intrusion volume. The particle size distribution of the crystalline lactose determined from the first intrusion run is shown in Fig. 3A, curve A. A satisfactory agreement is found with the particle size distribution measured by the air jet sieving technique (curve D, Fig. 3A).

If a second and a third mercury intrusion run are carried out on the same lactose sample after evacuation to extrude the already filled mercury, curves B and C (Fig. 2A) are obtained. Although the shape of these curves is very similar to that of the first run, the final intrusion volume is smaller, probably due to a different packing of the lactose powder particles caused by the first intrusion of mercury or to a partial entrapment of mercury. At any rate, by using the L'/A values derived from the porosities calculated by the second and third intrusion runs (ϵ = 0.38 and ϵ = 0.35, respectively), particle size distributions (curves B and C, Fig. 3A) are obtained which are practically superimposable with the curve derived from the first intrusion run.

Microcrystalline Cellulose—Microcrystalline cellulose is a powder well known for its intraparticle microporosity (37). Thus, it is interesting to study the applicability of the mercury porosimetry technique for particle size determination (based on the interparticle porosity) on this type of powder. Figure 2B shows the mercury intrusion curves into the microcrystalline cellulose powder. For all the intrusion runs, there is only one sharp penetration in a very low and restricted range of pressures (1–10 kg/cm²), which can be reasonably attributed to interparticle void intrusion. In fact, this low pressure range corresponds (*via* the Washburn equation) to a void size range of 8–0.8 μm, whereas the intraparticle pore sizes are <0.003 μm (37), the lowest pore size detectable by the porosimeter.

Thus, it is possible also in this case to apply the Mayer and Stowe approach to derive the particle size distribution of microcrystalline cellulose. The porosity values (0.68 for the first run, 0.60 for the second and third runs) derived from the intrusion curves and the mercury contact angle (145°) were used to obtain the particle size distributions shown in Fig. 3B. There is a good agreement between the mercury porosimetry (curves A, B, and C) and the electrical sensing zone technique (curve D), but this agreement is particularly good for the second and third runs (curves B and C). A tentative explanation may be the presence of a few aggregates in the microcrystalline cellulose powder, which could be eliminated by the first mercury intrusion. This interpretation can be further substantiated by carrying out porosimetry determinations on highly aggregated powders.

Aggregated Powders—In the case of lactose, no particular care was taken for the first or subsequent mercury intrusion runs in order to obtain porosimetry-derived particle size distributions comparable with the air jet sieving. But, particular attention must be paid when powder samples with aggregates are examined and when other reference techniques are used (*e.g.*, the electrical sensing zone method, which requires the dispersion of the sample into a suspension liquid prior to the test). In fact, mercury porosimetry tests are carried out directly on the powder samples in the dry state; consequently, mercury is forced not only between single

Table I—Mercury–Powder Contact Angles

Powder	Mercury Contact Angle
Povidone, cross-linked	154°
Magnesium stearate	152°
Barium sulfate	149°
Indoprofen	147°
Microcrystalline cellulose	145°
Lactose	144°
Morpholine derivative (drug A)	140°
Ergoline derivative (drug B)	140°
Fumed silica	136°

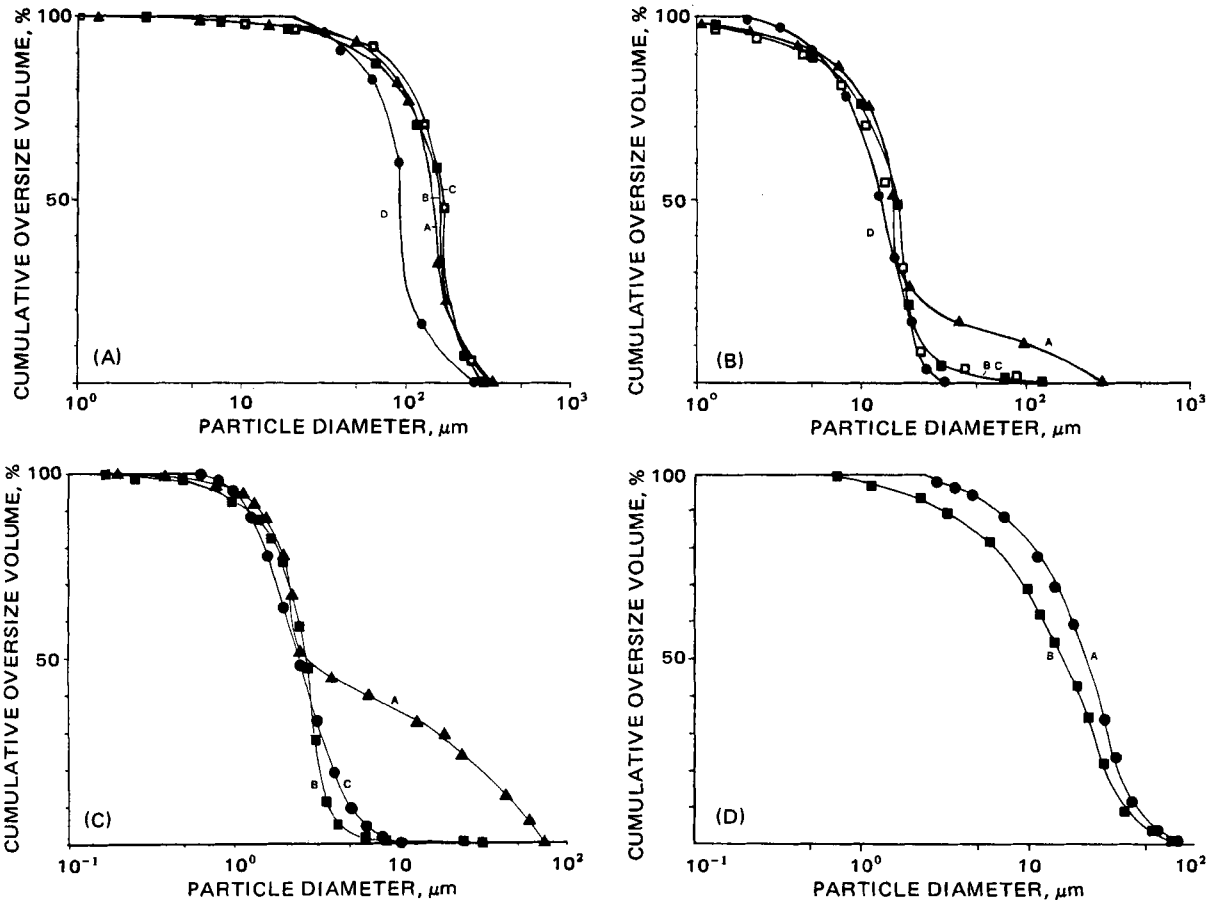

Figure 3—*Particle size distribution of crystalline lactose (A), microcrystalline cellulose (B), indoprofen (C), and magnesium stearate (D) powders. Key: (▲) derived from the first mercury intrusion run; (■) derived from the second intrusion run; (□) derived from the third intrusion run; (●) derived by air jet sieving (A) or electrical sensing zone method (B–D).*

particles, but (if present) also between aggregates and bundles of particles. If this is the case, particle size distributions derived by mercury porosimetry will differ from those derived by the electrical sensing zone technique after dispersion and sonication of the sample.

This point is illustrated by curves A and B in Fig. 2C (mercury intrusion curves) and Fig. 3C (particle size distributions) for the powdered drug indoprofen. The particle size distribution for indoprofen derived by mercury porosimetry (curve A, Fig. 3C) shows the presence of a high percentage of particles >10 μm, which are not detected by the particle counter method (curve C, Fig. 3C). This can be attributed to the presence of large aggregates in the dry indoprofen powder sample, which are eliminated by the dispersion and sonication techniques used prior to the electrical counting. If this interpretation is correct, disaggregation of the powder sample in the case of mercury porosimetry should eliminate the presence of larger particles. This is indeed the case, as shown by curve B in Fig. 3C, which was derived by a second mercury intrusion run (curve B, Fig. 2C) on the same indoprofen sample after evacuation to extrude the already filled mercury. In the first run (curve A, Fig. 2C), at low intrusion pressures (0.1–10-kg/cm^2 range) interaggregate voids are penetrated, whereas at higher pressures (20–50-kg/cm^2 range) both interparticle and intraaggregate penetration takes place, the latter leading to disaggregation of the powder, so that particle size distribution derived by a second mercury intrusion run is practically superimposable with that derived by the electrical sensing zone method. A third mercury intrusion run (curve C, Fig. 2C) showed no further change in the particle size distribution, suggesting that complete disaggregation of the powder samples is achieved after the first run and that no irreversible deformation of particles is caused by mercury intrusion.

Another example of this aggregation effect is given in Fig. 2D, showing porosimetry data for a magnesium stearate powder. In this case also, the second mercury intrusion run (curve B, Fig. 2D) greatly differs from the first run (curve A, Fig. 2D), indicating the presence of aggregates; in fact, if particle size data are derived only from the second mercury intrusion

Table II—Influence of Mercury–Powder Contact Angle on Particle Size Measurement

Powder	Particle Size at 50% Level, μm: Porosimetry, Calc. by Standard Contact Angle[a]	Porosimetry, Calc. by Experimental Contact Angle	Reference Technique[b]
Indoprofen	2.1	2.7 (147°)	2.5
Magnesium stearate	12.0	17.0 (152°)	21.0
Barium sulfate	1.7	2.1 (149°)	2.1

[a] 130°. [b] Electrical sensing zone.

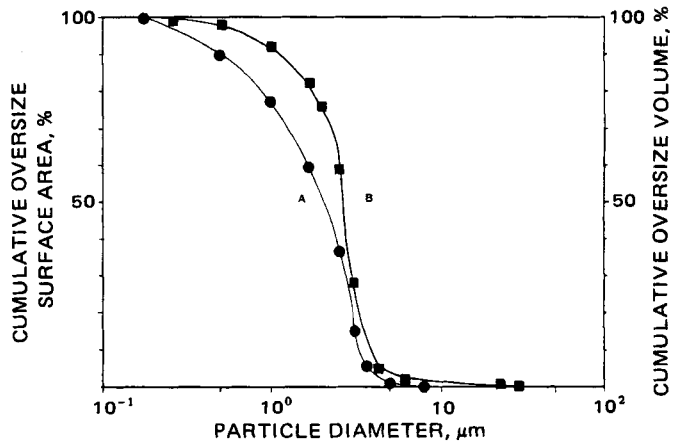

Figure 4—*Surface area distribution of indoprofen powder. Key: (●) surface area distribution derived from mercury intrusion, second run; (▲) particle size distribution derived from mercury intrusion, second run.*

Table III—Precision of Particle Size Analysis by Mercury Porosimetry: Reproducibility of Cumulative Oversize Volume Percentage Distribution Data of Morpholinic Derivative Drug A

Mercury Intrusion Pressure, kg/cm²	Particle Size, μm	Sample I, %	Sample II, %	Sample III, %	Sample IV, %	Sample V, %	Sample VI, %	Mean	*CV*, %
5	7.3	9.6	11.0	11.3	10.9	10.5	9.7	10.5	6.7
8	4.6	35.5	38.9	36.8	38.3	36.6	35.7	37.0	3.7
10	3.7	59.3	63.6	61.1	62.8	60.7	60.1	61.3	2.7
15	2.5	82.7	84.4	85.3	86.4	84.9	84.5	84.7	1.4
25	1.5	95.2	95.9	95.4	95.6	94.9	94.2	95.2	0.6

run (curve B, Fig. 3D) one can obtain a particle size distribution very similar to that derived by the electrical sensing zone method (curve A, Fig. 3D).

Influence of the Mercury–Powder Contact Angle—In previous papers showing particle size distributions derived by mercury porosimetry, standard contact angles of 130° (16, 18) or 140° (17) were used. The need for an experimentally measured value for each powder tested is illustrated in Table I, showing the large range of contact angle values found for a miscellaneous series of powders of pharmaceutical interest: from 154° for cross-linked povidone to 126° for fumed silica. Mercury contact angles influence the derived particle size data, as the value of the term L'/A in Eq. 2 is a function also of the contact angle itself (29). Table II stresses this point, showing that agreement between particle sizes at the 50% level measured by different techniques is improved by employing the experimentally measured contact angle instead of a standard value.

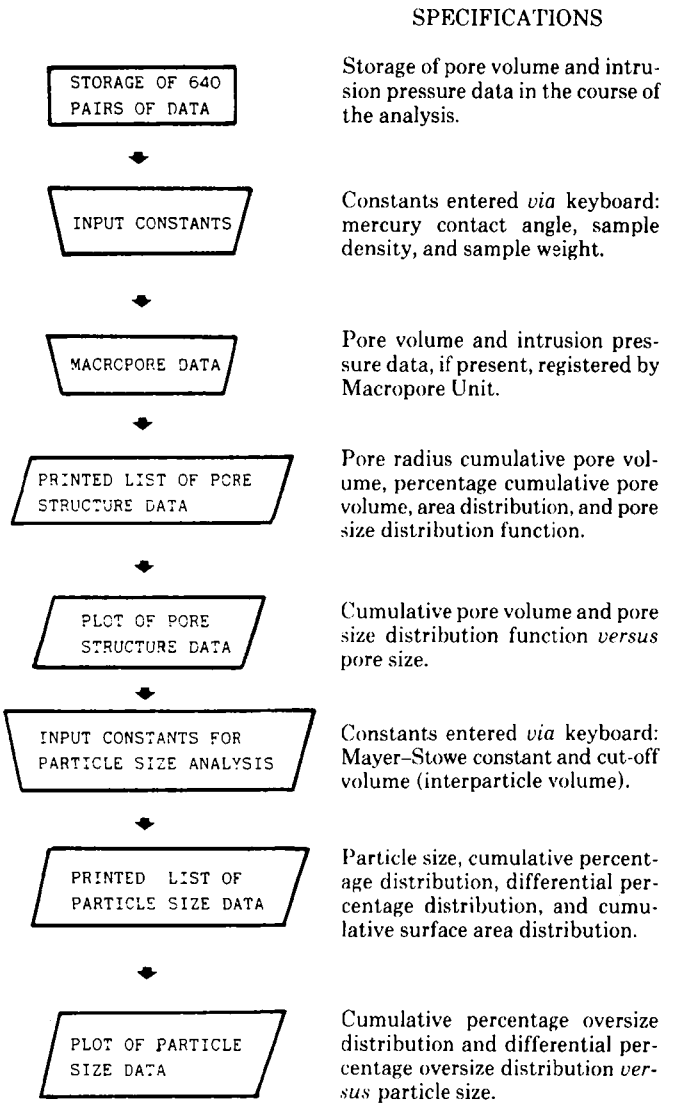

Scheme I—Flow diagram of microcomputer program for pore structure, surface area, and particle size analysis by mercury porosimetry.

Precision of the Method—Once the accuracy of the particle size distribution data derived by mercury porosimetry is optimized by taking into account the aggregation and contact angle effects, the precision of the method can be checked by carrying out many analyses on the same powder sample. Table III shows cumulative oversize volume percentage data of porosimetry analyses on samples of the morpholinic derivative (drug A). The data showed a very good reproducibility over the whole intrusion pressure range examined. The *CV* at any intrusion pressure is ≤3–6%, quite comparable with that usually found for a very reproducible method such as the electrical counting technique (typical *CV* of electrical counting data are usually <5–7%).

Surface Area Distribution Analysis—As shown in the theoretical considerations, at each intrusion pressure it is possible to derive a surface area value *via* Eq. 3. If this calculation is carried out over the whole intrusion pressure range and the surface area data are plotted against the particle sizes derived from the intrusion pressures, a surface area distribution on a particle size basis is obtained.

Figure 4 shows surface area distribution data (curve A) for the indoprofen powder, derived from curve B of Fig. 2C; the total surface area value is 3.38 m²/g. It is interesting to compare the surface area distribution (curve A) with the particle size distribution also reported in the same plot (curve B): the shape of the two curves differs quite notably in the small size range, indicating that smaller particles contribute much more to the overall surface area than to the volume distribution. For example, 24% (on a volume basis) of particles <2.0 μm originate 50% of the surface area, or 7% (by volume) of particles <1.0 μm originate 21% of the surface area.

As already outlined in the theoretical considerations, no geometrical assumption has to be made on the shape of the particles. In the electrical sensing zone method, surface area values are not experimentally measured, but simply calculated from the particle sizes assuming particle sphericity. From data in Table IV it appears quite evident that the geometrical approach can give only a rough estimate of the actual surface area. This observation is reinforced by comparing the total surface area values derived by porosimetry and electrical counting with the values found with another independent method such as the gas diffusion technique. As shown in Table IV, there is a fairly satisfactory agreement between porosimetry and gas diffusion, whereas electrical sensing zone data are lower. The particularly low surface area value derived by electrical counting for drug B is due to the presence of a large number of particles smaller than the minimum size detectable by this technique.

Microcomputer Program—The porosimeter is connected *via* an interface unit to a microcomputer and a printer–plotter. In the course of the analysis the microcomputer can store up to 640 pairs of data of intrusion pressures and mercury penetration volumes. At the end of the run, calculations are carried out as shown in the flow-chart presented in Scheme I. The main outputs of the program are: (*a*) printed lists of pore

Table IV—Comparison Between Mercury Porosimetry and Other Techniques of Surface Area Analysis

Powder	Specific Surface Area, m²/g: Porosimetry	Electrical Sensing Zone Method	Gas Diffusion
Indoprofen	3.38	2.13	2.93
Ergolinic derivative (drug B)	5.10	0.72	5.49
Magnesium stearate	1.48	0.40	1.80
Povidone, cross-linked	0.55	—[a]	0.84

[a] Not measured due to the swelling characteristics of the material.

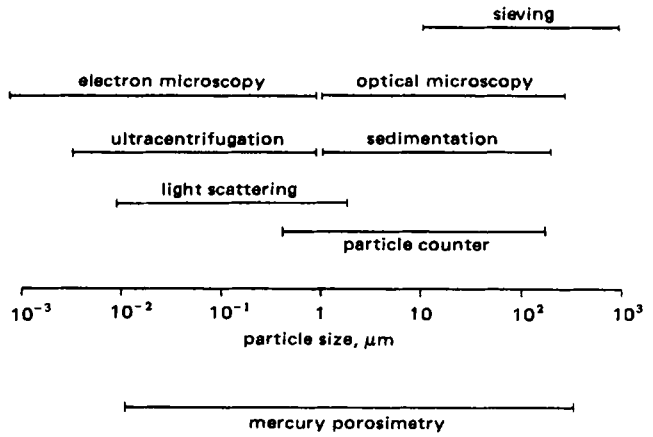

Figure 5—*Range of particle size measurement by different techniques.*

structure data, (*b*) plots of cumulative pore volume and pore size distribution functions, (*c*) printed lists of particle size and surface area analyses, and (*d*) plots of percentage cumulative and differential particle size distributions.

The program can be applied not only to powders with no intraparticle pores (as usually is the case with pharmaceutical powders), but also to porous powders. In fact the operator, after the pore structure data are fully printed and plotted, may decide to proceed to the particle size calculation. To do this, the operator must introduce, *via* the keyboard, the values of the Mayer–Stowe parameter and the "cut off" volume, *i.e.*, the found total interparticle void volume, which has to be distinguished from the intraparticle pore volume (18).

CONCLUSIONS

Mercury porosimetry can be a valuable method for deriving particle size distributions of pharmaceutical powders. Once the possible aggregation of the sample has been eliminated and the mercury contact angle has been measured, very good correlation is found between particle size data derived by mercury porosimetry and by other standard techniques. The basic advantages of the mercury porosimetry technique can be summarized as follows:

1. No particular treatment of the powdered samples is required. Powders are examined as received, in the dry state; this leads to a reduction in operator fatigue and time. Furthermore, possible damage or modification of the physical state of the sample caused by any treatment prior to the test, such as sonication, is ruled out.

2. As the powders are examined in the dry state, no limitation or trouble is posed by the solubility or swelling characteristics of the material. Highly soluble or swellable excipients (lactose, starch, powdered surfactants, *etc.*) can be analyzed easily.

3. A very wide range of particle sizes can be measured (Fig. 5). The upper particle size limit is given by the minimum intrusion pressure that can be exerted on the sample, usually given by the hydrostatic pressure of the mercury column. For example, for a mercury contact angle of 140° and a powder bed porosity of 0.36, the largest measurable particle size is 485 μm. The lower particle size limit is given by the maximum intrusion pressure which can be exerted by the porosimeter. For a maximum pressure of 2000 kg/cm^2, a mercury contact angle of 140°, and a powder bed porosity of 0.36, the smallest measurable particle size is 0.032 μm. This means that submicron powders can be analyzed with the same technique used for coarse powders, a major advantage over all other existing methods.

4. A surface area distribution on a particle size basis can be derived by the same mercury porosimetry analysis, requiring no additional experiment or apparatus. Furthermore, the surface area measurement is based on no geometrical assumption about the shape of the particles, allowing the derivation of an effective surface area comparable with data obtained by other experimental methods.

On the other hand, among the minor disadvantages of the technique, we should mention: (*a*) the possible difficulty in completely disaggregating some powder samples (although in the 30 powder samples we have examined thus far, this was never the case), (*b*) the assumption, only for the particle size derivation, that particles are spherical, as considered by the Mayer–Stowe model, and (*c*) the fact that particle size distribution data can be expressed only on a volume basis and not on a number basis. These minor limitations are furthermore reduced if we consider that practically all the existing particle size analysis methods, including the electrical sensing zone method or light scattering (8), make some assumptions on the particle geometry and that the volume or mass distribution is considered the most informative data for particle sizes of pharmaceutical powders. It must be stressed that particle sizes measured by mercury porosimetry are only indirectly derived from the data of interparticle void penetration, by assuming well-defined particle packing systems. This may pose severe problems with powder samples whose packing behavior (*e.g.*, needle-shaped particles or anomalous flow properties) cannot be interpreted by the classical theory.

On the whole, the advantages of the technique clearly outnumber the disadvantages, offering to workers in the physical pharmacy and pharmaceutical technology areas a new method of analyzing the particle size and the surface area distributions of powders. Furthermore, extension and application of the method to the qualitative or quantitative assessment of the degree of aggregation of powders caused by any process, such as micronization, is possible.

REFERENCES

(1) N. Watari, M. Hanano, and N. Kameniwa, *Chem. Pharm. Bull.*, **28,** 2221 (1980).

(2) N. Kameniwa, N. Watari, and H. Iijima, *Chem. Pharm. Bull.*, **26,** 2603 (1978).

(3) B. F. Johnson and J. O'Grady, *Br. J. Clin. Pharmacol.*, **5,** 465 (1978).

(4) J. T. Fell and J. M. Newton, *J. Pharm. Sci.*, **60,** 1866 (1971).

(5) N. A. Orr, Particle Size Analysis Conference, Loughborough, England, 1981.

(6) A. W. Hölzer and J. Syögren, *Int. J. Pharm.*, **2,** 145 (1979).

(7) Proceedings of the Symposium "Influenza Degli Eccipienti Sulla Cessione del Farmaco," BASF, Milan, 1979.

(8) T. Allen, "Particle Size Measurement," 2nd ed., Chapman and Hall, London, 1970.

(9) L. J. Beaubien and A. J. Vanderwielen, *J. Pharm. Sci.*, **69,** 651 (1980).

(10) A. E. Butcher and T. M. Jones, *J. Pharm. Pharmacol.*, 245, 1P (1972).

(11) P. V. Allen, P. D. Rahn, A. C. Sarapu, and A. J. Vanderwielen, *J. Pharm. Sci.*, **67,** 1087 (1978).

(12) C. F. Lerk, G. K. Bolhuis, and S. S. Smedema, *Pharm. Acta Helv.*, **52,** 33 (1977).

(13) S. M. Brown and E. W. Lard, *Powder Technol.*, **9,** 187 (1974).

(14) A. A. Liabastre and C. Orr, *J. Colloid Interface Sci.*, **64,** 1 (1978).

(15) H. M. Rootare and C. F. Prenzlow, *J. Phys. Chem.*, **71,** 2733 (1967).

(16) C. Orr, *Powder Technol.*, **3,** 117 (1969/70).

(17) M. Svata and Z. Zabranky, *Powder Technol.*, **3,** 296 (1969/70).

(18) N. G. Stanley-Wood, *Analyst*, **104,** 97 (1979).

(19) D. Sixsmith, *J. Pharm. Pharmacol.*, **29,** 82 (1977).

(20) H. Gucluyildiz, G. S. Banker, and G. E. Peck, *J. Pharm. Sci.*, **66,** 407 (1977).

(21) F. Carli, I. Colombo, L. Simioni, and R. Bianchini, *J. Pharm. Pharmacol.*, **33,** 129 (1981).

(22) W. D. Opankule and M. S. Spring, *J. Pharm. Pharmacol.*, **28,** 508 (1976).

(23) W. D. Opankule and M. S. Spring, *J. Pharm. Pharmacol.*, **28,** 806 (1976).

(24) R. C. Rowe, P. H. Elworthy, and D. Ganderton, *J. Pharm. Pharmacol.*, **25S,** 12 P (1973).

(25) F. Carli and L. Simioni, *Int. J. Pharm. Tech. Prod. Mfg.*, **2,** 23 (1981).

(26) P. J. Dees and J. P. Polderman, *Powder Technol.*, **29,** 187 (1981).

(27) E. W. Washburn, *Proc. Natl. Acad. Sci. USA*, **7,** 115 (1921).

(28) L. K. Frevel and L. J. Kressley, *Anal. Chem.*, **35,** 1492 (1963).

(29) R. P. Mayer and R. A. Stowe, *J. Colloid Sci.*, **20,** 893 (1965).

(30) L. G. Joiner, E. P. Barrett, and R. Skold, *J. Am. Chem. Soc.*, **73,** 3155 (1951).

(31) A. J. Goodsel, *Powder Technol.*, **9,** 191 (1974).

(32) G. L. Mack, *J. Phys. Chem.*, **40,** 159 (1936).

(33) R. E. Johnson and R. H. Dettre, "Surface Colloid Science," vol. 2, Wiley, New York, N.Y., 1969.

(34) S. Lowell and J. E. Shields, *J. Colloid. Interface Sci.*, **83**, 273 (1981).
(35) R. J. Good and R. S. Mikhail, *Powder Technol.*, **29**, 53 (1981).
(36) T. Allen and N. G. Stanley-Wood, *Powder Technol.*, **3**, 227 (1970).
(37) K. Marshall and D. Sixsmith, *Drug Dev. Commun.*, **1**, 51 (1974).

ACKNOWLEDGMENTS

Presented in part at the Particle Size Analysis Conference in Loughborough, UK (1981) and at the British Technology Conference in London, England (1982).

The authors thank M. Ulivieri for the electrical sensing zone measurements.

Liposome Disposition *In Vivo* VI: Delivery to the Lung

R. M. ABRA *, C. ANTHONY HUNT *[x], and D. T. LAU ‡

Received October 20, 1982 from the **School of Pharmacy* and ‡*Animal Care Facility, University of California, San Francisco, CA 94143.* Accepted for publication January 20, 1983.

Abstract □ The effect of negatively charged liposome components and vesicle size on the time course and dose dependency of liposome disposition in mice was studied with a view to optimizing liposome delivery to the lung. The disposition of large multilamellar liposomes was followed using ^{125}I-labeled *p*-hydroxybenzamidine phosphatidyl ethanolamine. Of the three negatively charged liposome compositions studied (phosphatidyl choline–X–cholesterol–α-tocopherol, molar ratio: 4:1:5:0.1; X = phosphatidyl serine, dipalmitoyl phosphatidic acid, or phosphatidyl glycerol), phosphatidyl serine liposomes resulted in the greatest accumulation in lungs. Lung levels decreased up to 95 h postdose, at which time 6% of the liposome dose present at 2 h still remained. The disposition of phosphatidyl serine-containing liposomes was independent of dose for the range 0.04–21 μmol/animal. When liposomes containing phosphatidyl choline were prepared using a variety of extrusion and dialysis conditions, a strong link between liposome size and lung accumulation was revealed. A maximum lung accumulation of 30.9% of the administered dose was achieved with no detectable gross pathological lung lesions up to 24 h postdose.

Keyphrases □ Liposomes—multilamellar, phosphatidyl serine, disposition *in vivo*, delivery to the lung, mice □ Disposition—multilamellar liposomes, *in vivo*, delivery to the lung, mice, phosphatidyl serine □ Phosphatidyl serine—multilamellar liposome disposition *in vivo*, delivery to the lung, mice

Liposomes may act as drug carriers (1, 2) but some degree of target specificity is necessary to maximize the therapeutic index of the drug. Intravenously administered liposomes generally become associated with organs of the reticuloendothelial system, mainly the liver and spleen (3, 4).

The lungs, because of their susceptibility to disease, *e.g.*, metastatic cancer (5), are a suitable target organ for attempts to localize drugs. Liposome preparations in common use generally do not accumulate in the lung to any significant extent after intravenous administration (6, 7). It is known, however, that liposome doses containing vesicles of ≥1-μm diameter exhibit improved localization in the lungs compared with smaller diameter preparations (8–10). This effect has been attributed to simple mechanical trapping in the capillary bed of the lungs (9). Liposomes bearing either positive (11) or negative (6, 10) surface charge accumulate in the lungs to a greater extent than neutral liposomes of similar size. However, there is some evidence that positively charged liposomes containing stearylamine may be toxic *in vivo* (12). Attempts have been made to deliver liposomes to the lungs *via* routes other than a distant intravenous site, *e.g.*, the ear vein of rabbits (13) and intratracheal instillation (14). Such approaches can have only specialized applications.

We have examined the effects of negatively charged liposome components and vesicle size on the time course and dose dependency of liposome disposition with a view to optimizing liposome delivery to the lungs. These results will be utilized for directing antitumor drugs to the lungs.

EXPERIMENTAL

Chemicals—Purified egg yolk phosphatidyl choline and phosphatidyl glycerol were prepared as previously described (15). Phosphatidyl serine[1], sodium dipalmitoyl phosphatidate[2], cholesterol[2], and α-tocopherol[2] were chromatographic grade. The method of Szoka and Mayhew (16) was used to synthesize the ^{125}I-labeled *p*-hydroxybenzamidine phosphatidyl ethanolamine (45 mCi/mg), subsequently referred to as the ^{125}I-marker. All other chemicals were at least reagent grade. The phosphate-buffered saline (pH 7.4) contained 92 mM sodium chloride, 43 mM anhydrous dibasic sodium phosphate, 11 mM monobasic sodium phosphate monohydrate, 100 USP U of penicillin, and 100 μg of streptomycin/mL. All buffer-containing solutions were routinely filtered through 0.22-μm pore size filters[3]. Dipalmitoyl phosphatidic acid was prepared by chloroform extraction of the sodium phosphatidate in 0.4 M HCl in 20% (v/v) methanolic aqueous solution.

Preparation of Liposomes—Liposomes were prepared as described previously (4). Three lipid compositions were used: (A) phosphatidyl choline, dipalmitoyl phosphatidic acid, cholesterol, and α-tocopherol; (B) phosphatidyl choline, phosphatidyl serine, cholesterol, and α-tocopherol; and (C) phosphatidyl choline, phosphatidyl glycerol, cholesterol, and α-tocopherol. In each case the molar ratio was 4:1:5:0.1. Sufficient lipid together with ~0.05 μCi of ^{125}I-marker per experimental animal was dried and suspended in buffer by mechanical agitation, yielding large multilamellar liposomes. In most cases these liposomes were subsequently extruded through polycarbonate membranes[4] having 8-, 5-, 3-, 2-, and 1-μm diameter pore sizes to generate populations having different mean diameters (17).

Liposomes were dialyzed at 4°C in the dark against frequent changes of buffer, for ~2 d. Dialysis was carried out in 1-mL dialysis cells fitted with 25-mm polycarbonate membranes[5] with a variety of pore sizes (specified below) to remove traces of dialyzable iodine-125 and some liposomes of smaller diameter than the membrane pores (17).

The final total lipid concentration was estimated by phosphorus assay (18) of extracted samples (19) and then corrected for the presence of non-phosphorus-containing lipids. Vesicle diameters were examed by electron microscopy following negative staining (4).

[1] Avanti Biochemicals Inc., Birmingham, Ala.
[2] Sigma Chemical Co., St. Louis, Mo.
[3] Millipore Corp., Bedford, Mass.
[4] Bio-Rad Labs, Richmond, Calif.
[5] Nucleopore, Bio-Rad Labs, Richmond, Calif.

0022-3549/84/0200-0203$01.00/0